Published in final edited form as:

*ASAIO J.* 2020 May ; 66(5): 572–579. doi:10.1097/MAT.0000000000001017.

# A Model of Pediatric End-Stage Lung Failure in Small Lambs <20 kg

**Benjamin D. Carr**[1,2], **Clinton J. Poling**[1], **Pavel Hala**[1,3,4], **Matias Caceres Quinones**[1,5,6], **Aaron R. Prater**[1], **Jennifer S. McLeod**[1,2], **Robert H. Bartlett**[1], **Alvaro Rojas-Pena**[1,6], **Ronald B. Hirschl**[1,2]

[1]Extracorporeal Life Support Laboratory, Department of Surgery, Michigan Medicine, University of Michigan, Ann Arbor, Michigan, USA

[2]Department of Pediatric Surgery, Michigan Medicine, University of Michigan, Ann Arbor, Michigan, USA

[3]Department of Cardiology, Homolka Hospital, Prague, Czech Republic, Department of Physiology, Charles University, Prague, Czech Republic

[4]Department of Pediatric Anesthesia, Hospital Luis Calvo Mackenna, University of Chile, Santiago, Chile

[5]Department of Anesthesia, Clínica Las Condes, Santiago, Chile

[6]Department of Surgery, Section of Transplantation, Michigan Medicine, University of Michigan, Ann Arbor, Michigan, USA

## Abstract

One in five children with end-stage lung failure (ESLF) die while awaiting lung transplant. No suitable animal model of ESLF exists for development of artificial lung devices for bridging to transplant. Small lambs weighing 15.7±3.1 kg (n=5) underwent ligation of the left anterior pulmonary artery (PA) branch, and gradual occlusion of the right main PA over 48 hours. All animals remained hemodynamically stable. Over seven days of disease model conditions, they developed pulmonary hypertension (mean PA pressure 20±5 vs 33±4 mmHg), decreased perfusion ($SvO_2$ 66±3 vs 55±8%) with supplemental oxygen requirement, and severe tachypneic response (45±9 vs 82±23 breaths/min) (all $p<0.05$). Severe right heart dysfunction developed (TAPSE 13±3 vs 7±2 mm, fractional area change 36±6 vs 22±10 mm, EF 51±9 vs 27±17%, all $p<0.05$) with severe tricuspid regurgitation and balloon-shaped dilation of the right ventricle. This model of pediatric ESLF reliably produces pulmonary hypertension, right heart strain, and impaired gas exchange, and will be used to develop a pediatric artificial lung.

CORRESPONDING AUTHOR: Alvaro Rojas-Pena, Extracorporeal Life Support Laboratory, B560, MSRB II, SPC5686, 1150 W. Medical Center Dr., Ann Arbor, MI 48109, +1-734-615-5357, alvaror@med.umich.edu.

CONFLICTS OF INTEREST:

The authors have no conflicts of interest to disclose.

### Keywords

Pediatric; Lung failure; Transplant; Bridge to transplant; Animal model; Ovine; Disease model; Pulmonary hypertension; Right heart failure; Echocardiography

## INTRODUCTION:

One in five children with end-stage lung failure (ESLF) die while awaiting lung transplant, and waitlist mortality is increasing.[1] Despite advances in other organ replacement therapies such as hemodialysis and ventricular assist devices, no bridge therapy to lung transplant exists.[2,3] The ideal bridge therapy would permit patients to be awake, spontaneously breathing, extubated, and ambulatory while awaiting transplant, and may even serve as destination therapy for those who are not transplant candidates. Such a device would also serve as destination therapy for patients whose underlying disease is expected to improve or resolve within one to two years as the lungs grow, such as bronchopulmonary dysplasia or congenital diaphragmatic hernia. This role is best filled by a para-corporeal artificial lung.[2,4]

Despite encouraging progress in adult artificial lung technology, device development for the pediatric population is sorely needed.[3] As experience with cardiac support therapies has shown, the unique challenges of pediatric translation are more complex than simply fabricating smaller versions of adult devices.[5] The requirements for priming volume, blood flow, gas exchange, and pressure drop in a device designed for a small child are necessarily far removed from those required for an adult, and without meticulous design toward pediatric applications, these devices are unlikely to succeed clinically. Thus, it is imperative that artificial lungs be specially developed and optimized for small children.

To meet this need, a disease model of pediatric ESLF must be defined. An appropriate model should replicate the physiologic endpoints of disease: hypoxia, hypercapnia, pulmonary hypertension, and right heart strain.[6,7] Although our laboratory has developed such a model in larger sheep,[8,9] to date no artificial lung experimentation has been carried out in animals weighing less than 25–30 kg. Half of pediatric lung transplants among children 0–11 years are performed in children younger than six years of age,[1] who would be expected to weigh under 20 kg,[10] and this group is also at highest risk of death while awaiting transplant.[1] To make optimized device development possible for these most vulnerable patients, we now describe an ovine recovery model of pediatric ESLF in newly-weaned lambs as small as 11 kg, suitable for testing artificial lungs for small children.

## METHODS:

All protocols were approved by the University of Michigan Committee on Use and Care of Animals, and animals received humane care in accordance with the NIH Guide for the Care and Use of Laboratory Animals.[11]

### Surgical Procedure

Healthy, newly-weaned lambs weighing 10–20 kg (n=5) were anesthetized with intravenous propofol 7 mg/kg, intubated, and mechanically ventilated. General anesthesia was

maintained with inhaled isoflurane 1–3.5%. An arterial line was placed into the left common carotid artery, and a Swann-Ganz pulmonary artery catheter was placed into the main pulmonary artery (PA).

A left thoracotomy was performed at the fourth intercostal space. The anterior branch of the left pulmonary artery was occluded with a silk ligature. The pericardium was then opened, the main PA was skeletonized, and the ligamentum arteriosum was ligated and divided. An adjustable Rummel-style tourniquet was placed around the right pulmonary artery just distal to the bifurcation and tunneled to the skin, as previously described.[9] A perivascular flow probe was placed around the main PA. (Figure 1)

Baseline echocardiography was performed and hemodynamics were recorded. Thoracostomy tubes were placed and attached to −20 mmHg suction. A 0.5% bupivacaine intercostal nerve block was performed at ribs 3–7 and a local anesthetic catheter was implanted in the subcutaneous tissues. The chest was closed in layers, the lungs were recruited, and animals were weaned to extubation.

## Echocardiography

An echocardiographic system (Siemens Acuson Cypress) and cardiac probes (Acuson 7V3c and Acuson 3V2c) were used for standard transthoracic and invasive (during thoracotomy) measurements of the heart dimensions and function. Two-dimensional, Doppler, and M-mode measurements were taken under general anesthesia at two time points: 1) at baseline, before surgical instrumentation and 2) at conclusion, after 7 days of disease model conditions, just before euthanasia.

Images were acquired through intercostal windows on left side of the chest, providing analogous views to the human parasternal short-axis and long-axis views. A four-chamber view was obtained from the sub-xiphoidal position, and acquisitions of the great vessels were obtained with the chest open at thoracotomy. The right ventricle was measured during end-diastole in length, basal, midventricular and apical diameters (RV EDD). Its single plane area was measured during systole (RV ESA) and diastole (RV EDA). Right ventricular systolic function was assessed from measured tricuspid annular plane systolic excursion (TAPSE; a measure of longitudinal contractility), calculated fractional area change (FAC = (RV EDA - RV ESA) / RV EDA; a measure of cross-sectional contractility), and ejection fraction (EF). The presence of a patent foramen ovale was ruled out in all lambs.

## Postoperative Care

Animals were recovered and monitored in stanchion restraints under 24-hour observation. Food and water were provided *ad libitum*. Prophylactic gentamicin 2.5 mg/kg every eight hours and nafcillin 500 mg every six hours were administered intravenously throughout the experiment. Pain was controlled using intravenous flunixin 1 mg/kg every eight hours and 0.5% bupivacaine 1 mg/kg injected every six hours via the local anesthetic catheter throughout the experiment. Buprenorphine 0.3 mg every six hours was administered intravenously as needed, based on a formal pain assessment. Supplemental oxygen was provided via nasal cannula to maintain arterial oxygen saturation >90%. Blood gas

measurements were obtained every two hours for the first 48 hours, and every three hours thereafter. Animal health, vital signs, and hemodynamics were monitored hourly.

### Disease Induction and Study End Points

Beginning on the first post-operative day, the adjustable right PA tourniquet was gradually cinched by 25% every 12 hours until the right PA was 100% occluded. Thus, full occlusion of the right PA was achieved at 48 hours, decreasing the total pulmonary vascular bed to less than 50%, and causing pulmonary hypertension. (Figure 2) The 48 hours prior to achieving 100% occlusion were defined as disease model Induction Days One and Two. Baseline data was collected during the 12 hours prior to cinching. No cinching was performed if the animal was requiring more than 2 L/min supplemental oxygen, in which case cinching was delayed and further occlusion was re-attempted after 12 hours. Once the right PA was 100% occluded, data was collected for seven days, or until criteria for euthanasia were met: arterial oxygen saturation <90% despite 4 L/min oxygen for >4 hours; mixed venous oxygen saturation <30% despite 4 L/min oxygen for >4 hours; $P_aCO_2$ >60mmHg on two or more blood gases within six hours; lactate >10 mmol/L at any point or >5 mmol/L on two consecutive measurements; or significant respiratory distress.

### Conclusion Echocardiography and Euthanasia

After seven days of 100% right PA occlusion, or if criteria for euthanasia were met, animals were again sedated with propofol 7 mg/kg intravenously, and intubated and ventilated under general anesthesia as before. The thoracotomy incision was re-opened and invasive echocardiography performed. The animal was then euthanized by intravenous injection of pentobarbital (Vortech Pharmaceuticals, Dearborn, MI), and one tissue sample of each heart chamber and bilateral tissue samples from the medial periphery of the middle lung lobes were preserved in formalin and sent for histologic analysis. (Figure 2)

### Statistical Analysis

Statistical analysis was performed using STATA v15 (StataCorp LLC, College Station, TX), and data were expressed as *mean±standard deviation*. Paired Student's t-test was used to compare means, and $p<0.05$ was considered significant.

## RESULTS:

Lambs weighed 15.7±3.1 kg. Baseline vital signs and laboratory values were normal (Table 1). There was no evidence of systemic illness or disease apart from expected changes related to the disease model. All five lambs survived the duration of the experiment (seven days following 100% right PA occlusion).

### Pulmonary Arterial Pressure

Mean PA pressure at the beginning of the experiment was normal, and increased significantly over seven days of disease model conditions (from 20±5 to 33±4 mmHg, $p<0.01$). Mean arterial pressure, heart rate, and PA blood flow (cardiac output) remained stable throughout. (Figure 3)

### $CO_2$ Clearance

There was increased variability in $pCO_2$ readings after disease model induction. Average $PaCO_2$ increased from 33±3 to 40±6 mmHg ($p<0.05$) over the first three days, but respiratory rate increased almost two-fold over the course of the experiment (from 45±0 to 82±23 breaths/min, $p<0.05$), compensating for the increase in alveolar dead space and rising $PaCO_2$ by the fourth day. (Figure 4)

### Oxygenation

Over seven days of disease model conditions, there was a significant decrease in mixed venous oxygen saturation (from 66±3% to 55±8%, $p<0.01$). Arterial oxygen saturation and average $PaO_2$ remained stable with supplemental oxygen via nasal cannula as needed. (Figure 5)

### Right Heart Strain

Echocardiographic findings are summarized in Table 2. Compared to baseline, the right ventricle enlarged in all cross-sectional diameters (basal from 20±3 to 28±3 mm, midventricular from 15±4 to 24±3 mm, apical from 10±2 to 14±1 mm, all $p<0.05$), enlarged longitudinally (from 36±6 to 45±3 mm, $p<0.05$) and dilated to form an enlarged, balloon-shaped chamber with the most prominent dilation in the apical and midventricular diameters, with septal bowing into the left ventricle (Table 2). RV EDA increased from 5.1±1.3 to 9.9±1.6 $cm^2$ ($p<0.05$) and RV ESA from 3.3±1.0 to 7.7±1.1 $cm^2$ ($p<0.05$). Baseline mean RV free wall thickness was 3±1 mm and did not increase.

Right ventricular systolic function worsened significantly, with reduction in TAPSE from 13±3 to 7±2 mm, FAC from 36±6 to 22±10 mm, and EF from 51±9% to 27±17% (all $p<0.05$; Figure 6). Severe tricuspid regurgitation developed in all lambs, with mean estimated systolic pressure gradient across the valve of 48±12 mmHg and enlargement of the right atrium. Mean PA diameter increased from 15±3 at baseline to 19±3 mm, but this change was not statistically significant.

Unlike the RV, the left ventricle retained its normal contractility, but decreased in size (EDD from 32±4 to 25±4 mm, $p<0.05$), reflecting reduced filling from decreased preload and higher right-sided pressures with septal bowing.

### Histopathology

Findings are summarized in Figure 7. There were findings consistent with acute volume overload of the left pulmonary vasculature in the left lung: there was pulmonary edema and increased vascular leakage with alveolar fibrin and wall thickening, and thickening and disruption of the tunica media of small- to medium-sized arteries with smooth muscle hyperplasia, adventitial remodeling, and vascular endothelial cell hypertrophy.

The findings in the right lung were consistent with acute hypoxic alveolar damage: there was acute alveolar wall damage with interstitial fibrosis and remodeling; alveolar septae were thickened and edematous; and there was hypercellularity and consolidation of parenchyma

adjacent to bronchioles and arterioles of the lung, with accumulations of inflammatory cells, fibrin, and collagen filling alveoli.

In the right atrium, there was locally extensive edema in the right atrium separating myofiber bundles, consistent with right heart strain. In the RV, there were findings consistent with right heart strain and cardiac injury: multifocal zones of myofiber degeneration and mineralization within the papillary muscles, associated with hypertrophied interstitial cells, granulation tissue, and scant inflammatory cells. In the left atrium and ventricle, there was minimal reactive granulation tissue and scattered inflammatory cells at the epicardial surface, but no other identifiable lesions.

## DISCUSSION:

### Disease Model

An ideal disease model for testing pediatric artificial lungs must satisfy several key requirements. First, it must recapitulate the features of ESLF: hypoxia, hypercapnia, pulmonary hypertension, and right heart strain. Second, it must deliver a significant physiologic insult to the study animal, while permitting survival for chronic device testing. Third, it must be clinically applicable. A device that is successful in the context of the model should translate readily to clinical application with minimal adjustments. In particular, the size of the animal and the strategy for cannulation and attachment are of critical importance for successful translation.

### Pediatric Device Development and Attachment Configurations

To date, no practicable model of ESLF has been described in an appropriately-sized animal system. Only one device specifically designed for children has been tested, in sheep weighing 25–31 kg.[12] However, no disease model was used, the size of the animals was larger than the target patient population, and the device incorporated a mechanical blood pump designed to bypass the native lungs altogether in a right-atrium-to-aorta configuration. This approach risks insufficient perfusion to the native lungs for metabolic and endocrine functions, and blood trauma from the pump.[2,13]

Other authors have proposed PA-to-PA attachment, with a snare between the anastomoses to divert flow to the artificial lung.[14] This preserves full blood flow to the native lung, driven by the RV. However, this approach is problematic in small children because the size of the PA makes it difficult to place multiple grafts, and because it increases right heart strain, risking circulatory collapse in patients who already have pulmonary hypertension due to their underlying disease.[2,13,15–17] Although right-atrium-to-PA attachment for RV offloading has been proposed by several groups, it requires a mechanical pump, and has only been designed and tested in an adult-sized sheep model with no disease.[18–21]

Our group has previously described a model of ESLF in sheep up to 30 kg using ligation of the right pulmonary artery, and shown that artificial lung attachment in a PA-to-left-atrium configuration alleviates the resultant pulmonary hypertension in acute experiments.[22] This approach is advantageous because it places the artificial lung circuit in parallel with the native lung circulation, offloading the RV and improving cardiac function while avoiding a

mechanical pump.[2,4,13] Though RV offloading via PA-LA circuits has been demonstrated by our group in numerous studies in adult sheep using a variety of investigational devices, it has not been implemented in a chronic recovery disease model,[22–28] and has only been tested once in pediatric-sized animals.[22] Nevertheless, PA-LA attachment is the strategy used in all successful cases of clinical artificial lung use reported to date in both adults and children.[29–31]

## Options for a Chronic Model of Pediatric ESLF

We considered other models of ESLF including one in adult sheep with burn/smoke inhalation injury in which a PA-to-PA device was tested over five or seven days.[16,32] This model is not suitable for optimizing a pediatric artificial lung for bridging to transplant, due to acute systemic inflammation and high expected late mortality from extra-pulmonary causes. Our lab and others have reported embolic models of pulmonary hypertension in piglets or adult sheep, but these models take weeks to induce, require repeated resource-intensive embolization procedures, and in general, do not cause consistent and significantly impaired gas exchange.[23,33]

Thus, we initially attempted a chronic recovery model of ESLF using right PA ligation in 20–30 kg lambs.[8] However, animals undergoing sudden right PA ligation frequently failed to wean from mechanical ventilation after surgery, and often died of cardiorespiratory failure within four days.[8] We were concerned that right PA ligation synchronous with recovery from anesthesia and thoracotomy may have caused early demise. Therefore, we temporally separated the surgical intervention and recovery from the disease model induction. An adjustable Rummel-style tourniquet on the right PA allowed us to recover the animal from surgery, then occlude the right PA the following day. This resulted in excellent lung failure physiology and prolonged survival compared to the previous model, but only two of seven sheep survived the full seven days of testing, survivors had minimal RV strain, and the size of the animals was still too large (25–40 kg) for testing an infant-size device.[9]

Therefore, to create an effective, appropriately-sized model of pediatric ESLF for chronic artificial lung testing, we used freshly-weaned lambs as small as 11 kg (mean 15.7±3.1 kg). We increased the severity of the disease model by ligating the left anterior PA branch in addition to placing the right PA tourniquet, resulting in greater than 50% alveolar dead space. We also instituted a 48-hour protocol of gradual right PA occlusion, which avoided the abrupt hemodynamic changes associated with sudden occlusion.

## Outcomes

Mean PA pressure increased significantly after right PA occlusion, while PA flow, systemic arterial pressure, and heart rate remained constant. This reflects an isolated lesion in the PA vasculature causing pulmonary hypertension and RV strain, without hemodynamic instability. We also observed that mean PA pressure by the end of the experiment was 33±4 mmHg. Thus, assuming a normal LA pressure of 10 mmHg, the PA-LA gradient is expected to be approximately 23 mmHg, more than sufficient to drive adequate flows through a low-resistance device.[22]

Occlusion of the right PA and the anterior branch of the left PA also converted more than half of the lung volume to dead space, resulting in significant deficits in gas exchange. Consistent with previous studies, perfusion was impaired, with a significant decrease in mixed venous saturation, and supplemental oxygen was required to maintain target arterial oxygen saturation.[9] Mean $PaCO_2$ also increased significantly, though lambs did not remain hypercarbic due to a dramatic compensation in respiratory rate up to 82±23 breaths/min.

### Histopathology

As expected, histopathology demonstrated changes of volume and pressure overload in left lung vasculature, with vessel remodeling. Complementary lesions of ischemia were seen in the right lung. The right heart musculature appeared edematous and degenerate, while minimal changes were seen in the left heart. These findings are consistent with occlusion of the right PA, with the entire cardiac output diverted to the left lung.

### Echocardiography

Due to eccentric RV remodeling, FAC is preferred over ejection fraction to evaluate overall systolic function, and TAPSE is a well-established measure of RV longitudinal contractility. The change in all three parameters demonstrated significant systolic right heart dysfunction. There was also high-gradient tricuspid regurgitation consistent with well-developed right heart failure. Severe increase in RV afterload and physiological dead space caused a balloon-shaped RV dilation, loss of myocardial contractility, and eccentric remodeling.

### Limitations

This model is limited because it recapitulates the endpoints of disease, rather than inducing underlying disease. No single lung pathology such as bronchopulmonary dysplasia or cystic fibrosis is re-created. Instead, physiologic dysfunction is caused by occlusion of major pulmonary vasculature over a period of 48 hours. Thus, it does not mimic the exact pathology likely to be encountered in clinical scenarios. However, it does offer a generalizable approach for testing and optimizing pediatric artificial lung devices, independent of underlying disease.

### Summary

The features of ESLF can be created in lambs weighing 10–20 kg by occlusion of the right PA and the left anterior PA branch, with resulting pulmonary hypertension, right heart strain, and impaired gas exchange. Lambs can survive under disease model conditions for seven days. This model will be used to test and optimize pediatric artificial lung devices which are already under development. This work is a crucial step in improving survival and quality of life for small ESLF patients awaiting lung transplant or lung growth and recovery.

## ACKNOWLEDGEMENTS:

The authors acknowledge the efforts of Lisa Haynes and Mark Langley for their technical assistance, Megan Mitchell for illustration, Cindy Cooke for review and preparation of the manuscript, and the University of Michigan Undergraduate Research Opportunity Program. Supported by NIH R01 HD015434–35.

SOURCE OF FUNDING:

Supported by NIH R01 HD015434–35, and in part by the University of Michigan Undergraduate Research Opportunity Program (UROP).

## ABBREVIATIONS:

| | |
|---|---|
| **ESLF** | End-stage lung failure |
| **PA** | Pulmonary artery |
| **RV** | Right ventricle |
| **EDD** | End-diastolic diameter |
| **ESA** | End-systolic area |
| **EDA** | End-diastolic area |
| **TAPSE** | Tricuspid annular plane systolic excursion |
| **FAC** | Fractional area change |
| **EF** | Ejection fraction |

## REFERENCES:

1. Valapour M, Skeans MA, Smith JM, et al.: OPTN/SRTR 2015 Annual Data Report: Lung. Am J Transplant 17 Suppl 1: 357–424, 2017. [PubMed: 28052607]
2. Zwischenberger JB, Anderson CM, Cook KE, Lick SD, Mockros LF, Bartlett RH: Development of an implantable artificial lung: challenges and progress. ASAIO J 47 (4): 316–20, 2001. [PubMed: 11482477]
3. Skinner SC, Hirschl RB, Bartlett RH: Extracorporeal life support. Semin Pediatr Surg 15 (4): 242–50, 2006. [PubMed: 17055954]
4. Bartlett RH, Deatrick KB: Current and future status of extracorporeal life support for respiratory failure in adults. Curr Opin Crit Care 22 (1): 80–5, 2016. [PubMed: 26702599]
5. Griffith BP: Children are not necessarily “small” adults: the growing field of miniaturized mechanical circulatory support. J Heart Lung Transplant 30 (1): 9–11, 2011. [PubMed: 21145474]
6. Dishop MK: Paediatric interstitial lung disease: classification and definitions. Paediatr Respir Rev 12 (4): 230–7, 2011. [PubMed: 22018036]
7. Sweet SC: Pediatric lung transplantation. Proc Am Thorac Soc 6 (1): 122–7, 2009. [PubMed: 19131537]
8. Alghanem F, Davis RP, Bryner BS, et al.: The Implantable Pediatric Artificial Lung: Interim Report on the Development of an End-Stage Lung Failure Model. ASAIO J 61 (4): 453–8, 2015. [PubMed: 25905495]
9. Trahanas JM, Alghanem F, Ceballos-Muriel C, et al.: Development of a Model of Pediatric Lung Failure Pathophysiology. ASAIO J 63 (2): 216–222, 2017. [PubMed: 27832003]
10. Kuczmarski RJ, Ogden CL, Guo SS, et al.: 2000 CDC Growth Charts for the United States: methods and development. Vital Health Stat 11 (246): 1–190, 2002.
11. Guide for the Care and Use of Laboratory Animals 8th ed. Washington (DC), National Academies Press (US), 2011.
12. Liu Y, Sanchez PG, Wei X, et al.: Effects of Cardiopulmonary Support With a Novel Pediatric Pump-Lung in a 30-Day Ovine Animal Model. Artif Organs 39 (12): 989–97, 2015. [PubMed: 25921361]
13. Haft JW, Griffith BP, Hirschl RB, Bartlett RH: Results of an artificial-lung survey to lung transplant program directors. J Heart Lung Transplant 21 (4): 467–73, 2002. [PubMed: 11927224]

14. Lick SD, Zwischenberger JB: Artificial Lung: Bench Toward Bedside. ASAIO Journal 50 (1): 2–5, 2004. [PubMed: 14763484]
15. Scipione CN, Schewe RE, Koch KL, Shaffer AW, Iyengar A, Cook KE: Use of a low-resistance compliant thoracic artificial lung in the pulmonary artery to pulmonary artery configuration. J Thorac Cardiovasc Surg 145 (6): 1660–6, 2013. [PubMed: 23402692]
16. Lick SD, Zwischenberger JB, Alpard SK, Witt SA, Deyo DM, Merz SI: Development of an ambulatory artificial lung in an ovine survival model. ASAIO J 47 (5): 486–91, 2001. [PubMed: 11575823]
17. Lick SD, Zwischenberger JB, Wang D, Deyo DJ, Alpard SK, Chambers SD: Improved right heart function with a compliant inflow artificial lung in series with the pulmonary circulation. Ann Thorac Surg 72 (3): 899–904, 2001. [PubMed: 11570380]
18. Liu Y, Sanchez PG, Wei X, et al.: Right ventricular unloading and respiratory support with a wearable artificial pump-lung in an ovine model. J Heart Lung Transplant 33 (8): 857–63, 2014. [PubMed: 24746636]
19. Wang D, Zhou X, Lick SD, Liu X, Qian K, Zwischenberger JB: An ambulatory pulmonary and right heart assist device (OxyRVAD) in an ovine survival model. J Heart Lung Transplant 26 (10): 974–9, 2007. [PubMed: 17919615]
20. Wu ZJ, Zhang T, Bianchi G, et al.: Thirty-day in-vivo performance of a wearable artificial pump-lung for ambulatory respiratory support. Ann Thorac Surg 93 (1): 274–81, 2012. [PubMed: 22115337]
21. Zhou K, Niu S, Bianchi G, et al.: Biocompatibility assessment of a long-term wearable artificial pump-lung in sheep. Artif Organs 37 (8): 678–88, 2013. [PubMed: 23452221]
22. Alghanem F, Bryner BS, Jahangir EM, et al.: Pediatric Artificial Lung: A Low-Resistance Pumpless Artificial Lung Alleviates an Acute Lamb Model of Increased Right Ventricle Afterload. ASAIO J 63 (2): 223–228, 2017. [PubMed: 27861431]
23. Akay B, Reoma JL, Camboni D, et al.: In-parallel artificial lung attachment at high flows in normal and pulmonary hypertension models. Ann Thorac Surg 90 (1): 259–65, 2010. [PubMed: 20609788]
24. Haft JW, Alnajjar O, Bull JL, Bartlett RH, Hirschl RB: Effect of Artificial Lung Compliance on Right Ventricular Load. ASAIO Journal 51 (6): 769–772, 2005. [PubMed: 16340366]
25. Sato H, Griffith GW, Hall CM, et al.: Seven-day artificial lung testing in an in-parallel configuration. Ann Thorac Surg 84 (3): 988–94, 2007. [PubMed: 17720415]
26. Sato H, Hall CM, Lafayette NG, et al.: Thirty-day in-parallel artificial lung testing in sheep. Ann Thorac Surg 84 (4): 1136–43; discussion 1143, 2007. [PubMed: 17888959]
27. Schewe RE, Scipione CN, Koch KL, Cook KE: In-parallel attachment of a low-resistance compliant thoracic artificial lung under rest and simulated exercise. Ann Thorac Surg 94 (5): 1688–94, 2012. [PubMed: 22959566]
28. Skoog DJ, Pohlmann JR, Demos DS, et al.: Fourteen Day In Vivo Testing of a Compliant Thoracic Artificial Lung. ASAIO J 63 (5): 644–649, 2017. [PubMed: 28719441]
29. Hoganson DM, Gazit AZ, Boston US, et al.: Paracorporeal lung assist devices as a bridge to recovery or lung transplantation in neonates and young children. J Thorac Cardiovasc Surg 147 (1): 420–6, 2014. [PubMed: 24199759]
30. Patil NP, Mohite PN, Reed A, Popov AF, Simon AR: Modified technique using Novalung as bridge to transplant in pulmonary hypertension. Ann Thorac Surg 99 (2): 719–21, 2015. [PubMed: 25639425]
31. Schmid C, Philipp A, Hilker M, et al.: Bridge to lung transplantation through a pulmonary artery to left atrial oxygenator circuit. Ann Thorac Surg 85 (4): 1202–5, 2008. [PubMed: 18355495]
32. Zwischenberger JB, Wang D, Lick SD, Deyo DJ, Alpard SK, Chambers SD: The paracorporeal artificial lung improves 5-day outcomes from lethal smoke/burn-induced acute respiratory distress syndrome in sheep. The Annals of Thoracic Surgery 74 (4): 1011–1018, 2002. [PubMed: 12400738]
33. Noly PE, Guihaire J, Coblence M, Dorfmuller P, Fadel E, Mercier O: Chronic Thromboembolic Pulmonary Hypertension and Assessment of Right Ventricular Function in the Piglet. J Vis Exp (105): e53133, 2015. [PubMed: 26575833]

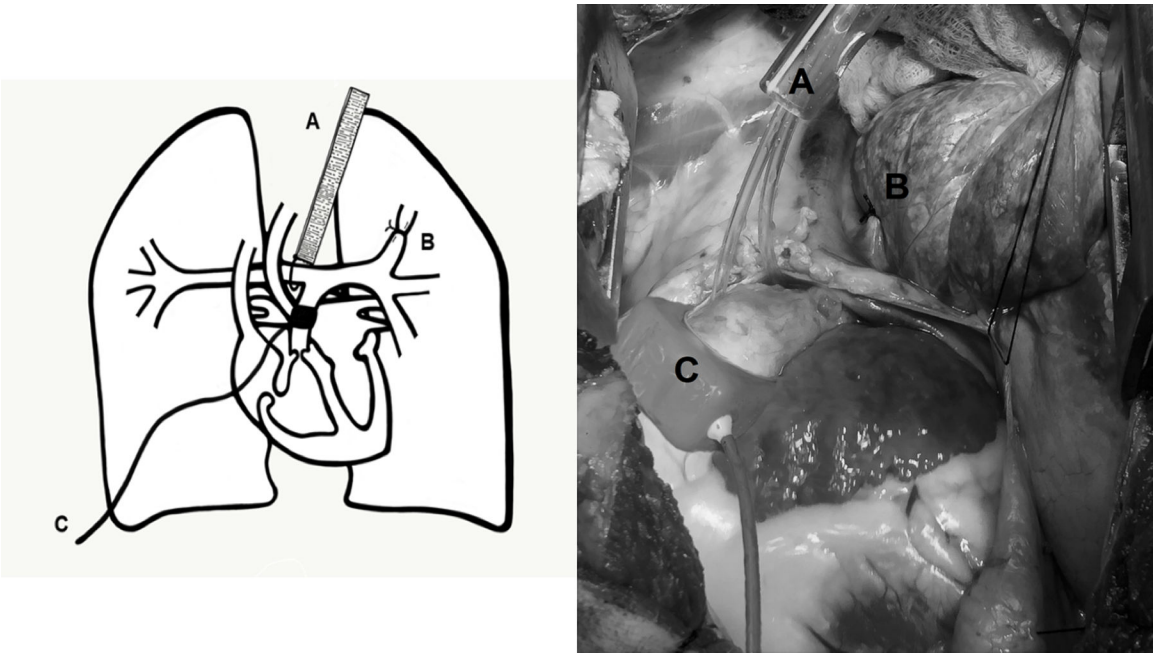


**Figure 1. Surgical Instrumentation, Diagram, And Intraoperative Photo**

A = Adjustable tourniquet controlling the right pulmonary artery; B = Ligated anterior branch of the left pulmonary artery; C = vascular flow probe around the main pulmonary artery.

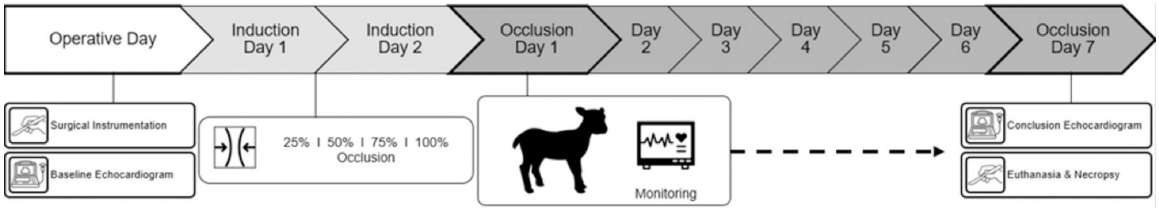


**Figure 2.**
Experimental Timeline

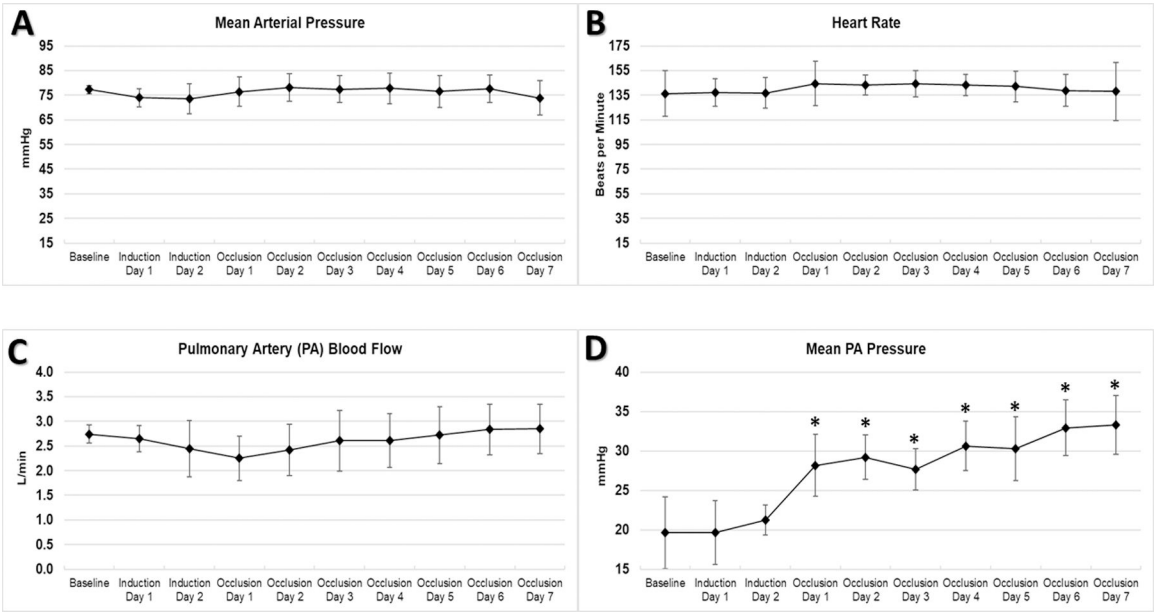


**Figure 3. Systemic Hemodynamics**

Mean arterial pressure (A), heart rate (B), and main PA flow (C) remained stable, while mean PA pressure (D) significantly increased after occlusion. * $p<0.05$ and ** $p<0.01$ compared to Baseline

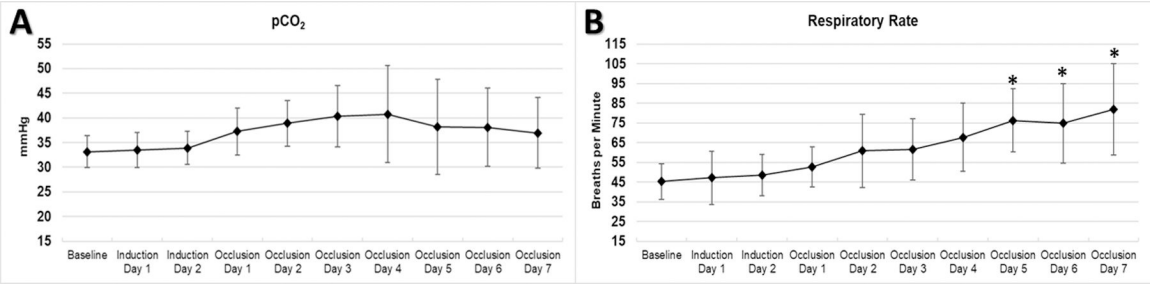


**Figure 4. Respiratory Variables (Ventilation)**

Animals experienced a transient increase in $pCO_2$ (A) and compensated with significantly increased respiratory rate (B). * $p<0.05$ and ** $p<0.01$ compared to Baseline

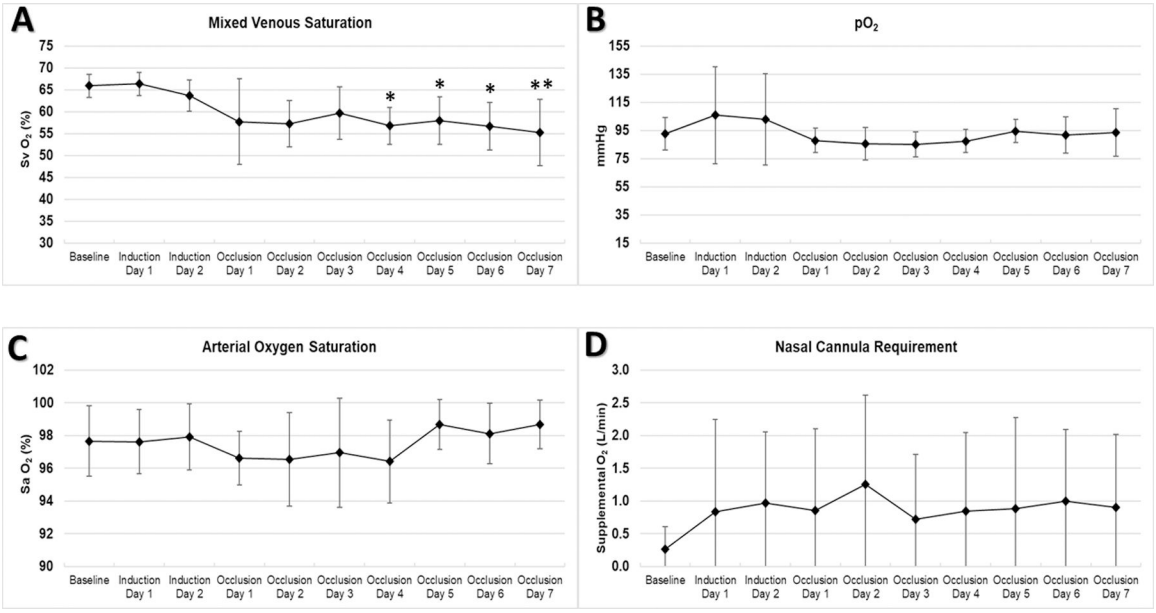


**Figure 5. Oxygenation and Oxygen Requirements**

Mixed venous saturation decreased significantly after occlusion (A), but $paO_2$ and oxygen saturation remained stable with supplemental $O_2$ via nasal cannula (B, C, and D). * $p<0.05$ and ** $p<0.01$ compared to Baseline

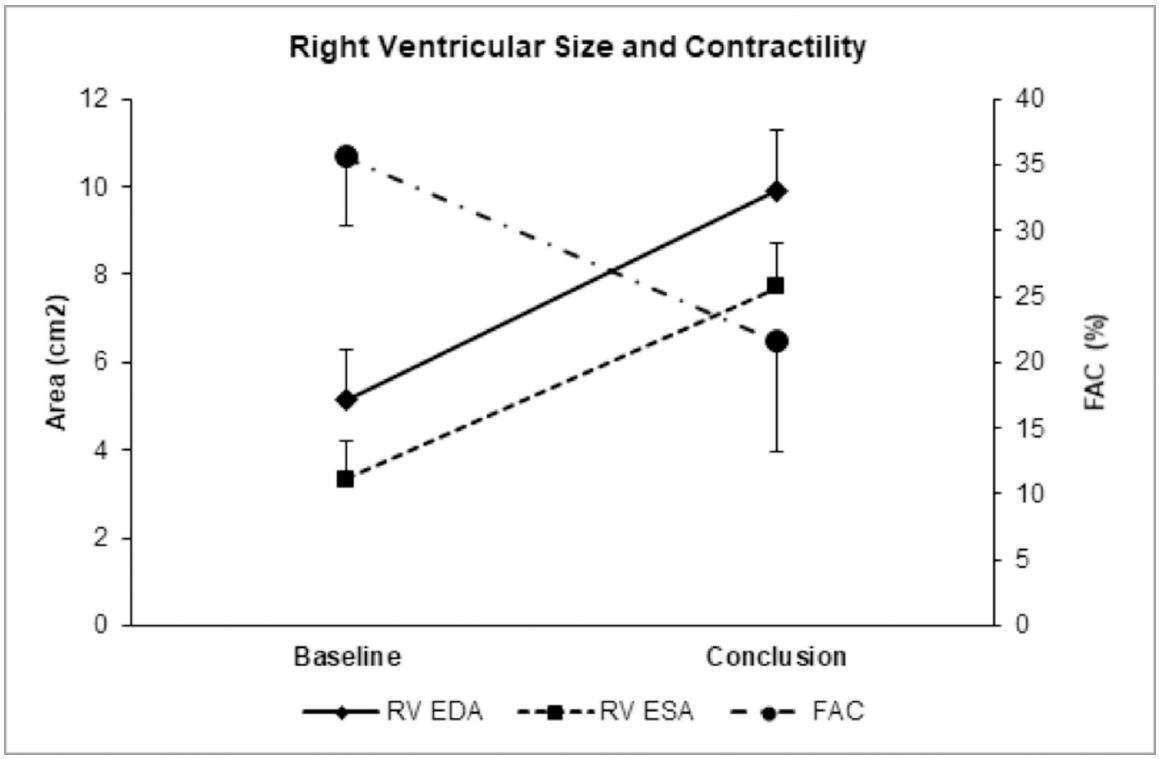


**Figure 6. Effects Of The Disease Model On Right Ventricular Function**

Over 7 days of 100% right pulmonary artery occlusion, right ventricular size significantly increased, while contractility significantly decreased ($p < 0.05$ for all parameters). RV EDA = right ventricular end-diastolic area; RV ESA = right ventricular end-systolic area; FAC = fractional area change

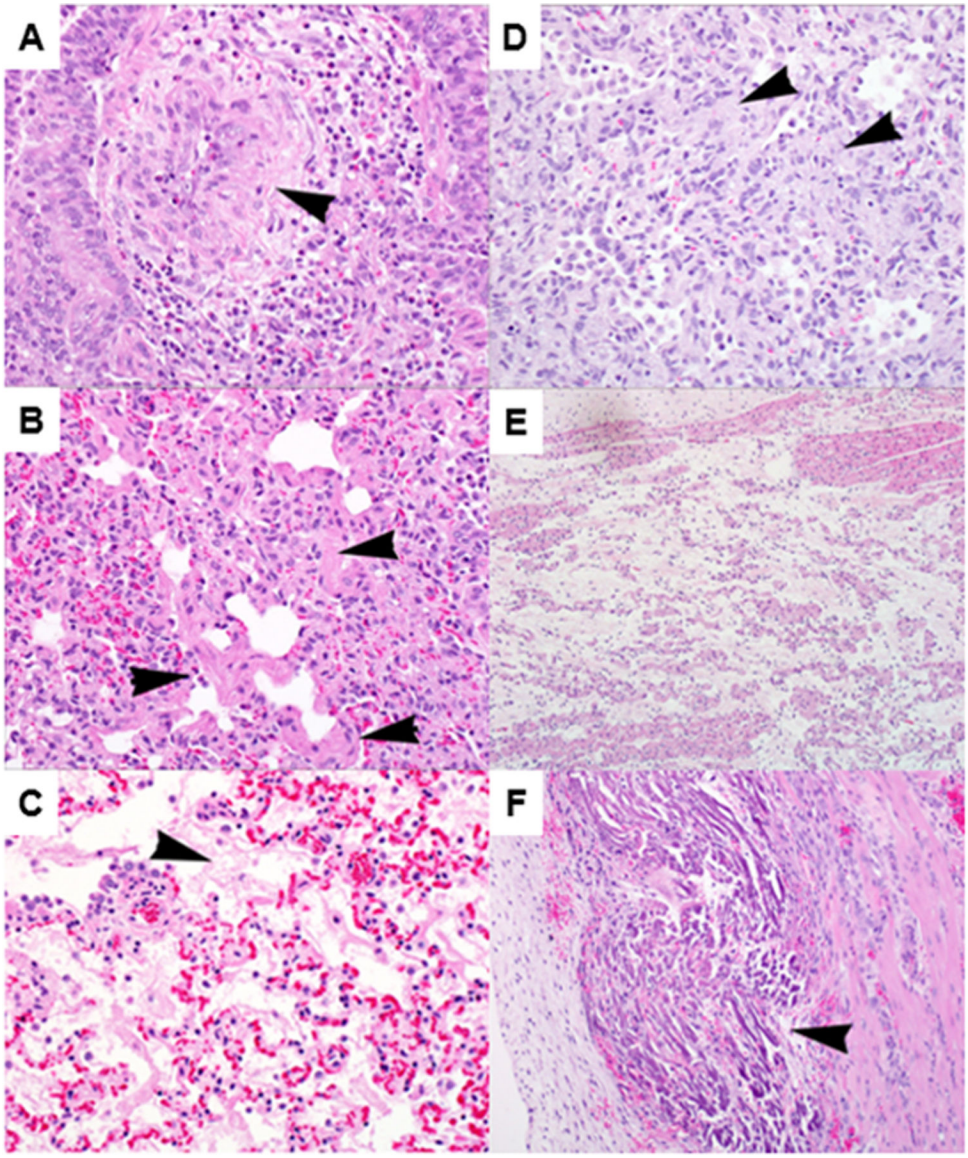


**Figure 7. Histology Of Lung And Cardiac Tissue**

Histologic findings of left lung (A and B), right lung (C and D), right atrium (E), and right ventricle (F). Left lung: thickening and disruption of tunica media of small arteries (arrowhead) with mixed perivascular inflammation (A); Left lung: smooth muscle hyperplasia (arrowheads) and focal interstitial fibrosis (B); Right lung: diffuse fibrin deposition in alveoli (arrowhead), and indistinct alveolar septae with diffuse congestion (C); Right lung: multifocal areas of acellular material (arrowheads), with edema and thickening of alveolar septae and alveolar spaces (D); Right atrium: locally extensive edema separating myofiber bundles (E); Right ventricle: multifocal zones of myofiber degeneration and mineralization within the papillary muscles (arrowhead), with hypertrophied interstitial cells, granulation tissue, and scant inflammatory cells (F).

**Table 1:**

Baseline characteristics of experimental lambs.

| Baseline Parameter (units) | Value |
|---|---|
| Weight (kg) | 15.7±3.1 |
| Heart Rate (beats/min) | 136±8 |
| Respiratory Rate (breaths/min) | 45±9 |
| Mean Arterial Pressure (mmHg) | 77±2 |
| Mean PA Pressure (mmHg) | 20±5 |
| pCO2 (mmHg) | 33±3 |
| pO2 (mmHg) | 93±12 |
| SaO2 (%) | 98±2 |
| WBC (K/uL) | 7±2 |
| Hemoglobin (g/dL) | 11±2 |
| Hematocrit (%) | 34±7 |
| Platelets (K/uL) | 638±128 |
| BUN (mg/dL) | 18±6 |
| Creatinine (mg/dL) | 0.5±0.1 |
| Albumin (g/dL) | 2.6±0.2 |

PA = pulmonary artery; WBC = white blood cells; BUN = blood urea nitrogen

**Table 2:**

Comparison of echocardiographic parameters at baseline and after 7 days of 100% right PA occlusion.

| Echocardiographic Parameter | Units | Baseline *(mean±standard deviation)* | Conclusion *(mean±standard deviation)* | Relative change *(%)* | p |
|---|---|---|---|---|---|
| **LV EDD** | mm | 32±4 | 25±4 | 79 | 0.03 |
| **RV EDD basal** | mm | 20±3 | 28±3 | 136 | 0.04 |
| **RV EDD midventricular** | mm | 15±4 | 24±3 | 166 | 0.03 |
| **RV EDD apical** | mm | 10±2 | 14±1 | 148 | 0.02 |
| **RV length** | mm | 36±6 | 45±3 | 125 | 0.02 |
| **TAPSE** | mm | 13±3 | 7±2 | 52 | < 0.01 |
| **PA diameter** | mm | 15±3 | 19±3 | 123 | 0.12 |
| **RV EDA** | $cm^2$ | 5±1 | 10±2 | 193 | 0.01 |
| **RV ESA** | $cm^2$ | 3±1 | 8±1 | 232 | 0.01 |
| **RV FAC** | % | 36±6 | 22±10 | 61 | 0.04 |
| **RV EF** | % | 51±9 | 27±17 | 53 | 0.03 |

LV = left ventricle; RV = right ventricle; PA = pulmonary artery; EDD = end-diastolic diameter; TAPSE = tricuspid annular plane systolic excursion; EDA = end-diastolic area; ESA = end-systolic area; FAC = fractional area change; EF = ejection fraction